Quantum Wireless Sensing: Principle, Design and Implementation

Fusang Zhang[†*], Beihong Jin[†*], Zitong Lan[†], Zhaoxin Chang[§†], Daqing Zhang[§♯], Yuechun Jiao[¶], Meng Shi[♮], Jie Xiong[‡]

[†] Institute of Software, Chinese Academy of Sciences, [*] University of Chinese Academy of Sciences, [§] Telecom SudParis, Institut Polytechnique de Paris, [♯] Peking University, [¶] Shanxi University, [♮] Technology and Engineering Center for Space Utilization, Chinese Academy of Sciences, [‡] University of Massachusetts Amherst
fusang@iscas.ac.cn, Beihong@iscas.ac.cn, zitonglan1@gmail.com, zhaoxin.chang@telecom-sudparis.eu, dqzhang@sei.pku.edu.cn, ycjiao@sxu.edu.cn, shimeng@csu.ac.cn, jxiong@cs.umass.edu

ABSTRACT

Recent years have witnessed a tremendous amount of interest in wireless sensing, i.e., instead of employing traditional sensors, wireless signal is utilized for sensing purposes. Contact-free wireless sensing has been successfully demonstrated using various RF signals such as WiFi, RFID, LoRa, and mmWave, enabling a large range of applications. However, limited by hardware thermal noise, the granularity of RF sensing is still relatively coarse. In this paper, instead of using the macro signal power/phase for sensing, we propose the first quantum wireless sensing system, which uses the micro energy level of atoms for sensing, improving the sensing granularity by an order of magnitude. The proposed quantum wireless sensing system is capable of utilizing a wide spectrum of frequencies (e.g., 2.4 GHz, 5 GHz and 28 GHz) for sensing. We demonstrate the superior performance of quantum wireless sensing with two widely-used signals, i.e., WiFi and 28 GHz millimeter wave. We show that quantum wireless sensing can push the sensing granularity of WiFi from millimeter level to sub-millimeter level and push the sensing granularity of millimeter wave to micrometer level.

CCS CONCEPTS

• **Human-centered computing** → **Ubiquitous and mobile computing**.

KEYWORDS

Quantum wireless sensing, Rydberg atom, Low system noise, Fine sensing granularity

ACM MobiCom '23, October 2–6, 2023, Madrid, Spain

ACM ISBN 978-1-4503-9990-6/23/10.
https://doi.org/10.1145/3570361.3613258

ACM Reference Format:
Fusang Zhang[†*], Beihong Jin[†*], Zitong Lan[†], Zhaoxin Chang[§†], Daqing Zhang[§♯], Yuechun Jiao[¶], Meng Shi[♮], Jie Xiong[‡] . 2023. Quantum Wireless Sensing: Principle, Design and Implementation. In *The 29th Annual International Conference on Mobile Computing and Networking (ACM MobiCom '23), October 2–6, 2023, Madrid, Spain.* ACM, New York, NY, USA, 15 pages. https://doi.org/10.1145/3570361.3613258

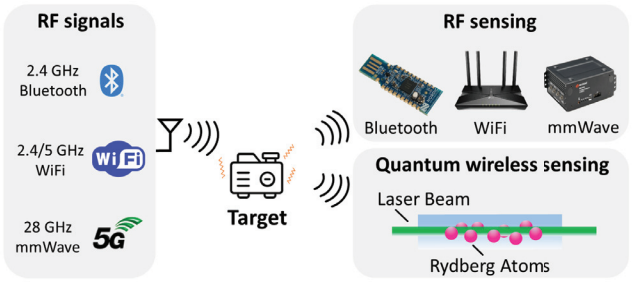

Figure 1: RF sensing vs. Quantum wireless sensing.

1 INTRODUCTION

Wireless technologies have changed our world and become an essential part of our everyday life. Besides the mainstream data communication function, in recent years, pervasive wireless signals such as WiFi are further exploited for sensing purposes [48, 62]. Owning to the nature of sensor free and contact free, wireless sensing has quickly attracted a lot of research attention with promising progress made [7, 36, 57]. A large range of applications have been realized including human gesture recognition [12, 42], vital sign monitoring [5, 26], vibration tracking [28, 53] and even material identification [22, 52]. While promising in many aspects, a key limitation associated with wireless sensing is the coarse sensing granularity. While WiFi sensing is capable of sensing hand gestures (i.e., a few centimeters of hand movement) and respiration (i.e., a few millimeters of chest displacement), it has difficulties in sensing heartbeat which

is on the scale of sub-millimeter. To achieve sub-millimeter sensing granularity, RF signals of higher frequencies (e.g., mmWave) need to be adopted. This is because the fundamental principle behind wireless sensing is that signal varies with target movement. For motion sensing, a phase rotation of 2π corresponds to a target movement of half signal wavelength. Therefore, sensing granularity is closely related to signal wavelength. For a specific target movement, a smaller signal wavelength indicates a larger signal phase variation which is easier to be detected.

The minimum phase variation that can be accurately captured is limited by the thermal noise of hardware. Conventional electronic components such as mixers, amplifiers, and analog-to-digital converters (ADCs) all unavoidably introduce thermal noise. Taking WiFi as an example, the widely used Intel 5300 WiFi card can report a minimum phase change of 15 degrees, corresponding to a target displacement of 3 mm. Therefore, WiFi sensing can hardly be used to track a movement smaller than 3 mm. Although higher-frequency signals can be utilized to achieve a finer granularity, higher frequency leads to larger signal strength attenuation and weaker penetration capability.

In this paper, as shown in Figure 1, we propose a new sensing modality, i.e., quantum wireless sensing for the first time. We show that quantum wireless sensing can significantly improve the sensing granularity by an order of magnitude. Recently, quantum technology has been exploited to enable quantum computing [37], quantum communication [25], quantum sensing [21], quantum routing [46] and quantum cryptography [39]. Note that quantum sensing in existing literature aims at capturing the information of micro subjects such as molecules [21, 56]. The typical examples are atomic vapor magnetometers and atomic clocks [19]. In contrast, the proposed quantum wireless sensing refers to sensing macro subjects such as human and daily objects.

As shown in Figure 2, the basic principle of a quantum receiver is that the electrons of an atom (e.g., Cesium atom) are triggered to higher energy levels to receive RF signals. For example, to receive 2.4 GHz WiFi signals, the electrons are triggered from energy level 6 to energy level 66. In quantum systems, an atom with electrons at high energy levels (i.e., above level 20) is called a *Rydberg atom* [23]. We observe several unique advantages of applying a quantum receiver [41] for sensing, compared to a conventional RF receiver.

- Quantum wireless sensing can achieve a much finer granularity. By using a quantum receiver for signal reception at WiFi frequency, the sensing granularity can be improved from 3 mm to 0.1 mm.
- Conventional RF receivers are designed to receive signals in a particular frequency range. Even the antenna needs to be redesigned in order to efficiently receive signals of different frequencies. Interestingly, in quantum wireless sensing, one quantum receiver can receive RF signals of different frequencies by simply triggering the electrons to different energy levels. One quantum receiver can easily cover frequencies from a few Megahertz to tens of Terahertz.
- Even for narrow-band WiFi signals, the frequency band still has a size of 20 MHz to 80 MHz. This causes interference between adjacent overlapping channels. In contrast, quantum wireless sensing only listens to a very small band, i.e., 0.05 MHz ~ 0.1 MHz, significantly reducing interference from adjacent channels.

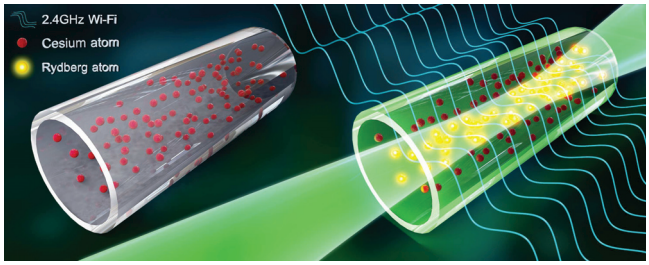

Figure 2: Quantum receiver. The Rydberg atoms are triggered to high energy level to receive RF signals.

The key reason quantum wireless sensing can achieve a finer granularity is that a quantum receiver does not contain electronic components such as mixers, amplifiers, and analog-to-digital converters (ADCs) inside a traditional RF receiver. A quantum receiver mainly contains atoms with electrons at different energy levels. Electrons at a particular level can capture signals within a particular frequency range (e.g., Cs atoms with electrons at the $66D_{5/2}$ energy level[1] can receive WiFi signal in the range of 2.39 GHz to 2.4 GHz). One observation is used to measure the strength of the received RF signal. That is, when RF signals are received at Rydberg atoms, the state of Rydberg atoms vary. When a laser beam penetrates through the vapor cell filled with Rydberg atoms, the change of Rydberg atom state causes the spectrum of the laser to vary. A stronger RF signal can cause a larger separation of the two peaks on the laser spectrum which can be measured by a photodetector [45] .

When a target moves, it affects signal propagation, causing signal strength variations which can be accurately captured at the quantum receiver. We theoretically model the effect of target motion on the measured quantum variation, revealing the principle behind quantum wireless sensing in detecting subtle signal change and accordingly subtle target motions. To further improve the sensing granularity, we adopt a reference signal design. Specifically, we leverage an interesting observation at quantum receiver, i.e., the laser spectrum peak

[1]Here, 66 indicates the main energy level and $D_{5/2}$ depicts the sub-level.

separation caused by RF signal reception is not linearly related to the signal strength [38]. The amount of separation is larger in the higher strength region. We therefore employ a reference RF signal to trigger the atom to a higher strength state. With this operation, the amount of target-induced peak separation change becomes much larger and accordingly the sensing granularity is significantly improved.

We implemented the first quantum wireless sensing prototype using a 2.5 cm atomic vapor cell filled with Cs atoms as a quantum receiver. This vapor cell filled with Cs atoms costs around $150 and the price can be significantly reduced under mass production. Experiment results show that the proposed quantum wireless sensing system can increase the sensing granularity by more than 10 times. We showcase that with such a high sensing granularity, 2.4 GHz RF signal can be used to capture the subtle vibration of a speaker on the sub-millimeter scale, which originally could only be achieved using high-frequency 60 GHz mmWave signals. We also show that with just one receiver, quantum wireless sensing can facilitate sensing with signals of different frequencies. For millimeter wave (28 GHz) signal, we demonstrate that quantum wireless sensing is able to sense micrometer-level vibration, enabling exciting applications such as recovering sound from the extremely subtle vibrations of a bottle induced by a small-size speaker. The main contributions of this paper are summarized as follows.

- We propose the concept of quantum wireless sensing for the first time. We introduce the underlying principle behind quantum wireless sensing, more specifically, why a quantum receiver is capable of achieving a finer granularity and how to leverage it for macro motion sensing.
- We design the first end-to-end quantum wireless sensing system including both the hardware design and the signal processing pipeline.
- We comprehensively evaluate the system performance with wireless signals of different frequencies. We show that compared with conventional RF sensing, quantum wireless sensing improves sensing granularity by an order of magnitude.

2 PRELIMINARY OF QUANTUM WIRELESS SENSING

In this section, we first introduce the basics related to quantum wireless sensing including the Rydberg atom and its electron transition with RF signals. Then we briefly present the RF sensing methodology.

2.1 Rydberg atom

Atoms are the smallest unit of matter, consisting of one nucleus and multiple electrons bound to the nucleus as shown in Figure 3. Electrons are bound to a specific set of orbits by the electromagnetic force of the nucleus. The electrons in each orbit have different energy levels.

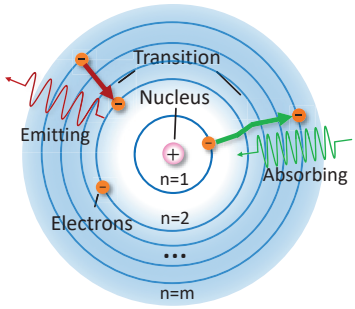

Figure 3: Illustration of atom structure and electron transition.

An electron that is further away from the nucleus has a higher energy. In physics, the principal quantum number n is used to represent the orbit index of an electron. At each orbit, the electron can also be in different energy levels. The energy level of an electron is determined by three quantum numbers. For example, $l = 66D_{5/2}$ represents an energy level, where $n = 66$ is the principal quantum number, D is the orbital angular momentum quantum number and 5/2 is the electron spin quantum number. The energy of an electron at an energy level l can be expressed as

$$E_l = -\frac{hcRy}{(n-\delta_l)^2}, \tag{1}$$

where h, c and Ry are Planck's constant, the speed of light and the Rydberg constant, respectively. δ_l is the quantum defect, which is a constant for each energy level.

An electron can "jump" between different energy levels, which is called *atomic electron transition* [3]. As shown in Figure 3, an electron can absorb energy to transit to higher energy levels, or it can release energy to transit to lower energy levels. Electrons absorb or release energy in the form of *receiving or emitting electromagnetic waves*. Note that both light signals and RF signals are electromagnetic waves. Since the energy of each energy level is determined, the frequency of electromagnetic waves absorbed (or emitted) due to the transition between two energy levels (e.g., l_1 and l_2) is determined as

$$f_{l_1 \to l_2} = \frac{|E_{l_1} - E_{l_2}|}{h}, \tag{2}$$

where E_{l_1} and E_{l_2} are the values of two energy levels, respectively. Based on this equation, for electrons at l_1 energy level, irradiating the atoms with electromagnetic waves of frequency $f_{l_1 \to l_2}$ causes electrons to transit to l_2 energy level.

A Rydberg atom is an atom with one or more electrons at high energy levels (i.e., above level 20). Rydberg atoms are created from ordinary alkali metal atoms (e.g., Rb and Cs

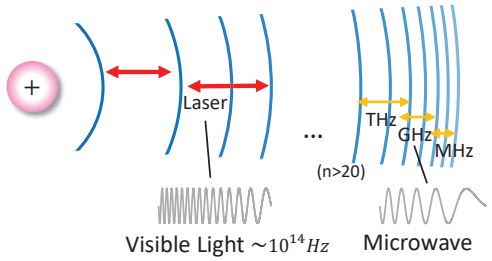

Figure 4: Illustration of energy levels.

atoms). The reason why alkali metal atoms are chosen is that they contain only one electron on the outermost level, which is easier to be triggered to higher energy levels. According to Equation 1, the energy of each level E_l is proportional to $-\frac{1}{n^2}$. The larger n is, the denser the energy levels are as shown in Figure 4. When n is large, the energy difference between nearby energy levels are small which corresponds to low-frequency wave according to Equation 2. The frequency can be on the scale of Megahertz to Terahertz. For example, the transition between energy levels $l_1 = 66D_{5/2}$ and $l_2 = 67P_{3/2}$ of Cs atom corresponds to RF signals at 2.4 GHz. So an absorption of WiFi signal of frequency 2.4 GHz can trigger the outermost electron to move from energy level $66D_{5/2}$ to $67P_{3/2}$. The calculation process is as follows

$$\begin{aligned} f_{l_1 \to l_2} &= \frac{|E_{l_2} - E_{l_1}|}{h} \\ &= cRy|\frac{1}{(67-\delta_{l_2})^2} - \frac{1}{(66-\delta_{l_1})^2}| \\ &= 2.4\ GHz, \end{aligned} \tag{3}$$

where $Ry = 1.097 \times 10^7 m^{-1}$, $c = 3 \times 10^8 m/s$, $\delta_{l_1} = 2.466$ and $\delta_{l_2} = 3.559$. The list of quantum defects [35] with various quantum numbers is attached as Appendix A.1. We also show how other signal frequencies such as 5 GHz and 28 GHz can be obtained with energy level transitions in Appendix A.2. In contrast, ordinary atoms have all the electrons located at low energy levels. The transition between low energy levels correspond to visible light signals, whose frequency is much larger (i.e., larger than 10^{14} Hz). Note that the energy difference between low energy levels is much larger.

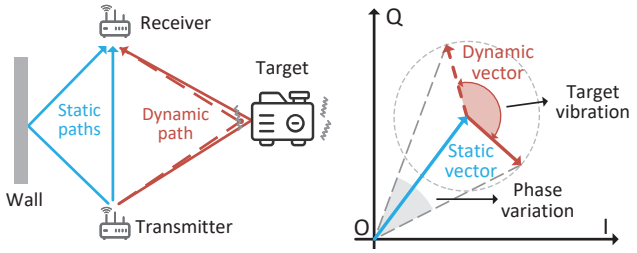

Figure 5: Principle of conventional RF sensing.

2.2 Conventional RF sensing

The basic principle of RF sensing is that target movement induces signal variations and we can therefore extract target context such as moving speed and distance through analyzing variations of the signal reflected from the target. As shown in Figure 5, an RF signal (e.g., WiFi signal) is emitted by a transmitter and then propagates through multiple paths to reach the receiver. Static paths denote those signal paths reflected from static objects (e.g., a wall). In contrast, dynamic path represents the path reflected from the target with motions. Both signal amplitude and phase variations can be used for sensing. As shown in Figure 5, signal amplitude and phase variations can be used to sense object vibration. On the I-Q plane, the static path vector is in blue color and the dynamic path vector is in red color. The composite signal at the receiver is the superposition of the two signal vectors. During the sensing process, the static vector does not change while the dynamic vector changes with target movements. The target vibration causes clear amplitude and phase variations of the dynamic vector. If we visualize the process on the I-Q plane shown in Figure 5, the dynamic vector rotates with respect to the static vector. The increase and decrease on the amplitude/phase of the composite vector correspond to target motions.

3 SYSTEM DESIGN OF QUANTUM WIRELESS SENSING

In this section, we present the detailed design of quantum wireless sensing.

3.1 System overview

As shown in Figure 6, the key difference between quantum wireless sensing and conventional RF sensing is that quantum wireless sensing uses a quantum receiver instead of an RF receiver to receive RF signals. RF transmitter first generates the baseband signal $e^{j2\pi f_0 t}$ and then mixes it with carrier frequency f_c. The transmitted signal can be represented as

$$S_T(t) = e^{j2\pi(f_c+f_0)t}. \tag{4}$$

Note that the transmitted signal arrives at the target and is

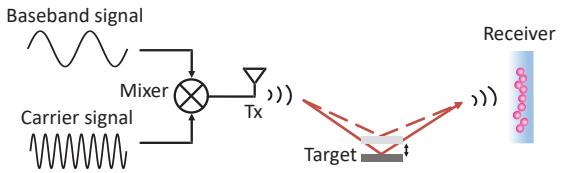

Figure 6: Illustration of quantum wireless sensing.

then reflected to the quantum receiver. Our goal is to quantify the effect of target motion on atoms at the quantum receiver and use the fine-grained atom state change for sensing.

3.2 Principle of quantum wireless sensing

Conventional RF sensing uses RF circuits to receive and demodulate signals. Specifically, the antenna captures RF signals and a mixer is used to demodulate the signal to baseband. Then, an ADC is used to sample the signal. In contrast, quantum wireless sensing exploits Rydberg atoms to receive the signal. Based on Section 2.1, to receive RF signals, the outermost electron needs to be triggered to high energy levels and the atom is called a Rydberg atom. We introduce how to generate Rydberg atoms next.

3.2.1 Rydberg atom preparation. Rydberg atoms are made from alkali metal atoms. The alkali metal atoms (i.e., Li, Na, K, Rb and Cs) contain only one electron at the outermost level, which is easier to be triggered to higher energy levels (e.g., from n = 6 to n = 66 for Cs) to reach the Rydberg state. As shown in Figure 7, a vapor cell is filled with Cs atoms with the outermost electrons at the ground state (i.e., $6S_{1/2}$). To excite the atoms to Rydberg state, two laser beams of different frequencies penetrate through the vapor cell from opposite directions [21]. The first laser beam triggers the outermost electron to the excitation state (i.e., from $6S_{1/2}$ to $6P_{1/2}$) and the second laser beam further triggers the electron to higher levels (i.e., from $6P_{1/2}$ to $66D_{5/2}$) and now the ordinary atom becomes a Rydberg atom. Besides the triggering function, the first laser serves another function, i.e., to be received by the photodetector to generate the laser spectrum which is used to measure the strength of the received RF signal.

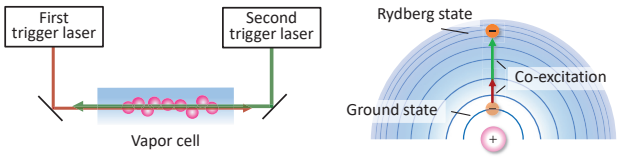

Figure 7: Exciting atoms to a Rydberg state.

3.2.2 Receive RF signals using Rydberg atoms. The energy levels of the Rydberg states are so dense that transitions between two states can induce RF signals with a fine-grained frequency resolution [3]. For example, the transition between $66D_{5/2}$ and $67P_{3/2}$ induces a 2.4 GHz RF signal, while the transition between $67D_{5/2}$ and $68P_{3/2}$ leads to a 2.3 GHz RF signal. Therefore, to use a Rydberg atom to receive an RF signal of frequency f_c, we need to find two energy levels (l_1 and l_2) between which the transition corresponds to an RF signal of frequency f_c. This can be obtained by traversing Equation 2. The atom will first be excited to energy level l_1 with laser beams. At l_1, the Rydberg atoms can absorb the energy of RF signals to transit to another energy level l_2 as shown in Figure 8 (left). Based on l_1 and l_2, we know the frequency (f_c) of the received RF signal. Another important parameter of the RF signal is the signal strength. To obtain this parameter, we leverage an interesting observation [45], i.e., the reception of RF signal results in a split of spectrum of the trigger laser beam and the signal strength is linearly related to the amount of split (Δf). The spectrum of the laser beam can be obtained using a photodetector. As shown in Figure 8 (right), the spectrum of laser beam shows one peak when there is no RF signal. When RF signal is captured at the quantum receiver, the peak of the spectrum is split into two. The quantitative relationship between the peak difference (Δf) of the spectrum and the strength of the RF signal is expressed as [45]

$$E = 2\pi \frac{h}{\mu} \frac{\lambda_p}{\lambda_c} \Delta f, \tag{5}$$

where λ_p and λ_c are the wavelengths of two laser beams and μ is a constant. Therefore, by measuring the amount of split of the two peaks on the spectrum, the strength of the RF signal can be calculated. The frequency range of the RF signal a Rydberg atom can receive at this energy level is $[f_c - \frac{B}{2}, f_c + \frac{B}{2}]$. B is around 100 kHz, implying that a quantum receiver has a much lower chance of being interfered with other signal sources due to the much smaller band.

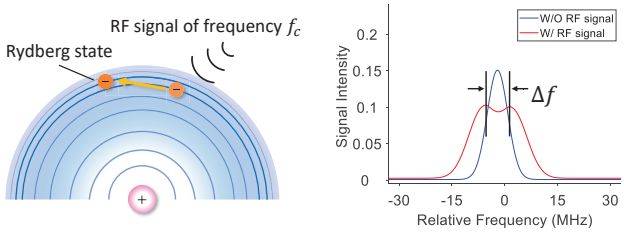

Figure 8: Left: receive RF signals; Right: the spectrum of first trigger laser beam w/ and w/o RF signals.

3.3 Sensing granularity enhancement with a reference signal

As illustrated in Section 3.2.2, the strength of the RF signal can be measured by the separation of the spectrum peaks. When signal strength varies, the amount of peak separation on the spectrum varies accordingly. We can therefore use the amount of peak separation to sense target motions. Note that the sensing granularity is now related to the amount of peak separation. For the same movement, a larger peak separation indicates a higher sensing granularity. To achieve a higher sensing granularity, we leverage an interesting observation of quantum receiver, i.e., the amount of separation is not linearly related to the signal strength [38]. We observe that the amount of separation is larger in the higher strength region. Therefore, we employ a reference RF signal to trigger the atom to the higher strength state. With this operation, the amount of peak separation change becomes much larger and accordingly the sensing granularity is significantly increased.

As shown in Figure 9a, without a reference signal to trigger the atom to a high strength state, the amount of spectrum

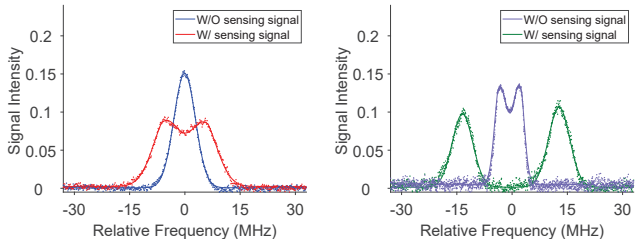

(a) w/o reference signal (b) w/ reference signal

Figure 9: Employ a reference signal to enhance sensing granularity.

peak separation change is pretty small. After the atom is triggered by a reference signal, the amount of peak separation change becomes larger for the same sensing signal change. We therefore employ a reference signal to increase the effect of target motion on spectrum peak separation to improve the sensing granularity.

3.4 Quantify the relationship between quantum effect and target motion

We have shown the relationship between target motion and the spectrum peak separation in Section 3.3. In Figure 10, we plot the peak separation induced by the displacement of subtle target vibration. The variation frequency of the peak separation matches the vibration cycle and we can therefore obtain the vibration frequency. However, in some applications, we care about not just the frequency but also the amount of vibration displacement, i.e., vibration amplitude. To further obtain the amount of vibration displacement, we need to mathematically quantify the rigorous relationship between target movement distance and the amount of peak separation change. We derive the relationship as below.

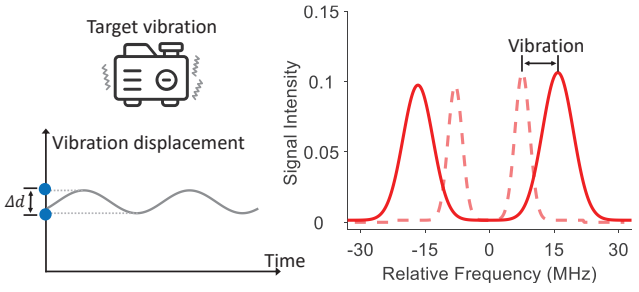

Figure 10: Illustration of relationship between target vibration (Left) and spectrum peak motion (Right).

The quantum receiver employs a photodetector to measure the amount of spectrum split (Δf) to obtain the strength of the received RF signal (E). Because the sensing signal $S_T(t)$ varies over time, the strength of detected sensing signal $E(t)$ also varies with time and can thus be represented as

$$E(t) = E_s cos(\omega_s t + \varphi_s), \tag{6}$$

where $\omega_s = 2\pi(f_c + f_0)$. It can be seen that the strength of the detected signal fluctuates over time at the frequency of $f_c + f_0$. According to Equation 5, the measured peak difference would also change over time at the frequency of $f_c + f_0$. In reality, the state of the Rydberg atom can not change that quickly and interestingly this inability serves the function of a mixer in a conventional RF receiver to remove the carrier frequency (f_c) and only keep the baseband (f_0) part. The actual signal strength detected at the quantum receiver can thus be expressed as

$$E(t) = E_s cos(\omega_0 t + \varphi_s), \tag{7}$$

where $\omega_0 = 2\pi f_0$. Based on Equation 7, when a target moves, E_s and φ_s change accordingly.

To accurately measure target movement distance, we need to obtain both values of E_s and φ_s. Existing works mainly extract phase information for quantum communication. For communication, accurate absolute phase information is required and an expensive reference oscillator is usually used. In contrast, in sensing, we only care about the relative phase change induced by target motions. In this case, the oscillator is not required and we now introduce the signal processing method to extract the phase change for sensing. To obtain φ_s, we multiply $E(t)$ by $cos(\omega_0 t)$ and its phase-shifted version $sin(\omega_0 t)$, respectively to form a complex value. We then use a low-pass filter (LPF) to remove the high-frequency component ($\omega_0 t$)

$$E'(t) = LPF\{E(t)cos(\omega_0 t) + j \cdot E(t)sin(\omega_0 t)\} = E_s e^{j\varphi_s}. \tag{8}$$

Now φ_s can be calculated as the angle of $E'(t)$: $\varphi_s = \angle(E_s e^{j\varphi_s})$. Let $\Delta\varphi_s$ denote the phase change caused by target movement. From a macroscopic perspective, conventional receivers receive RF signals using antennas. From the microscopic perspective, quantum receiver received RF signals using the electron energy transition of atoms. Based on the Schrödinger equation [23], $E'(t)$ can be measured in both macroscopic and microscopic perspectives. The difference is the measurement precision. Therefore, at the quantum receiver, the phase information of $E'(t)$ is also related to the path length of the received RF signal. We can thus convert the phase change to target displacement Δd as

$$\Delta d = \frac{c\Delta\varphi_s}{2\omega_s}. \tag{9}$$

Note that Equation 9 quantifies the relationship between phase change of the target-reflection signal and target displacement. In real-world scenarios, static objects in the environment such as walls also reflect signals. Thus, the signal strength detected at the quantum receiver also contains the strength of other signals. To deal with the non-target signals, we apply circle fitting [24] to remove those components in $E'(t)$.

3.5 Time-domain beamforming

In this section, we present a signal processing scheme to further improve the sensing granularity. It is known that the sensing granularity can be enhanced by increasing the Signal-to-Noise Ratio (SNR) [33]. One approach to improve SNR is spatial-domain beamforming [50], which constructively combines signals received at different antennas. Inspired by spatial-domain beamforming, we exploit time-domain "beamforming" [11, 20] to help increase sensing granularity in quantum wireless sensing. This is because the target moves at much lower frequencies (a few Hertz) compared to the signal sampling rate of photodetector (10 MHz). Therefore, adjacent samples contain very similar target movements but different noises. We can thus downsample the signal into multiple groups and combine them to increase the SNR.

As shown in Figure 11, we down-sample the collected signals $E'(t)$ into N groups. After performing time domain "beamforming", the fluctuation of the signal is more obvious. Based on our experiments, time domain beamforming can improve sensing granularity by around 20%. We next introduce the implementation of the quantum system.

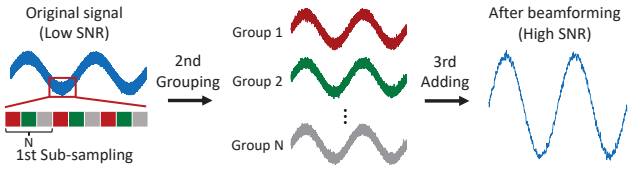

Figure 11: Time-domain "beamforming".

4 IMPLEMENTATION

Hardware Implementation. As shown in Figure 12a, one key component of the proposed quantum wireless sensing system is a cylindrical atomic vapor cell. The size of the vapor cell can vary and is usually small. In our experiment, the size of the cell is 2.5 cm × 5.0 cm, and it is filled with Cs atoms. The filled cell costs $150. The laser generator (Wavicle Laser ECDL852) used in our experiment costs $27,000. Note that this laser generator is capable of emitting laser in a large wavelength range, and it is thus expensive. For RF sensing with WiFi, UWB and millimeter wave, a cheaper laser generator suffices. For signals at 2.4 GHz frequency, two lasers of wavelength 510 nm and 852 nm are used to excite Cs atoms to the Rydberg state ($66D_{5/2}$) as shown in Figure 12b. Note that to receive signals at 5 GHz or 28 GHz, the corresponding Rydberg states are $52D_{5/2}$ and $61D_{5/2}$, respectively.[2] A photodetector (Thorlabs PDB210 A/M) is used to measure the laser intensity. Note that the photodetector does not need to be changed when the quantum receiver listens to different RF frequency bands. The detected light spectrum information is stored in a data acquisition board (NI USB-6363). We extract the frequency difference between the two peaks on the spectrum to calculate the strength of the received signal.

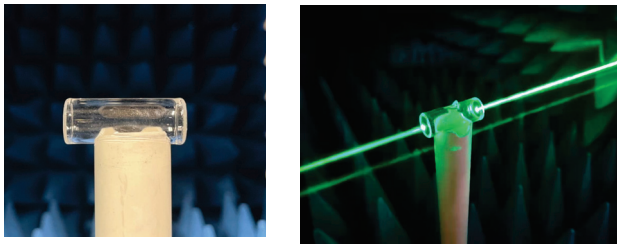

(a) Cs atoms at ground state **(b) Cs atoms at Rydberg state**

Figure 12: Two states of Cs atoms.

To generate RF signals over a large frequency range (e.g., 2.4 GHz, 5 GHz and 28 GHz), we employ a signal generator KEYSIGHT E8257D supporting frequencies up to 40 GHz. We also use commodity WiFi card as the transmitter to demonstrate quantum wireless sensing works with WiFi packets. The Intel 5300 WiFi card costs $18 and it was connected to a mini PC (GIGABYTE GB-BXi5-4570R) to control signal transmission. In the benchmark experiment, we use a vibration calibrator as the sensing target, which can generate vibrations with frequencies ranging from 15 Hz to 250 Hz and vibration amplitudes from 0.05 mm to 1 mm. For movement larger than 1 mm, we use a sliding track to precisely move a metal plate to serve as the target.

Software Implementations. We implement the signal processing part with Matlab. After the data acquisition card receives the raw signal samples, it forwards them to a laptop through WiFi connection. Then we employ the proposed signal processing and sensing granularity enhancement techniques to process the signal for sensing.

5 EVALUATION

In this section, we evaluate the performance of the proposed quantum wireless sensing system with both benchmark experiments and real-world applications. Benchmark experiments are employed to verify the feasibility of the proposed quantum wireless sensing system and investigate the impact of varying parameters and conditions. We further showcase two applications with the proposed quantum wireless sensing system: i) using a 2.4 GHz centimeter-wavelength signal to sense sub-millimeter level vibration of a speaker to "hear" the music play, and ii) using a 28 GHz millimeter-wavelength signal to sense micrometer-level subtle vibration of a water bottle induced by human walking.

5.1 Benchmark experiments

We evaluate the system performance in terms of vibration amplitude and frequency estimation accuracy. We compare

[2]We present the details of calculation in the Appendix.

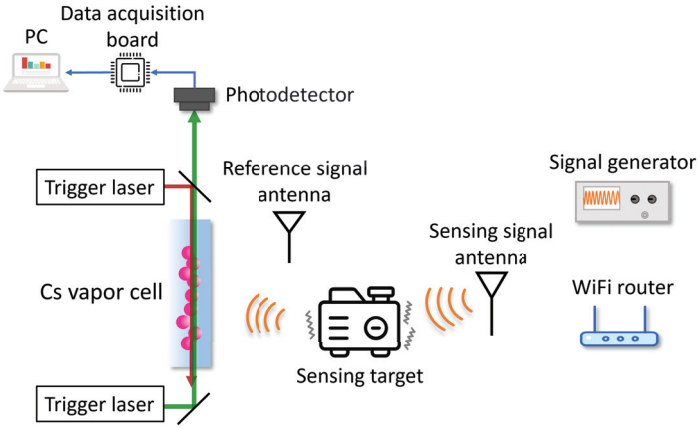

(a) Illustration of experiment setup

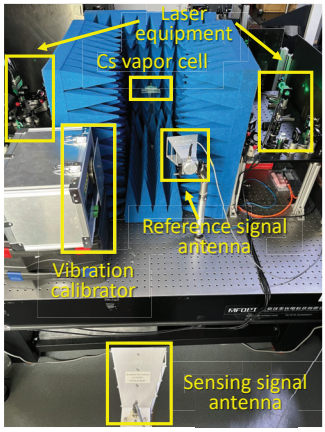

(b) Experiment setup in a real environment

Figure 13: Experiment setup.

the performance of the proposed quantum wireless sensing system with that of two state-of-the-art RF sensing systems [1][2]. We also evaluate the system performance in non-line-of-sight (NLoS) scenarios and in the presence of interference.

Experiment Setting: The experiment setup is shown in Figure 13. To fully control the target in the benchmark experiment, we use a small metal plate as the target. Real-life targets such as humans and speakers are adopted in the application evaluation section. The size of the metal plate is 10 cm × 15 cm. We employ a sliding track of 2 m controlled by Raspberry Pi 3 Model to precisely move the metal plate. The sliding track can move a target on a scale larger than 1 mm. For subtle vibration motions smaller than 1 mm, we employ a VEC-12 Portable Vibration Calibrator. The vibration displacement can be varied in the range of 10 - 2000 μm, and the frequency can be varied in the range of 10 - 800 Hz. By default, the target is placed 1 m away from the line-of-sight (LoS) path between the RF transmitter and quantum receiver. The RF transmitter and quantum receiver are separated by 2 m.

Ground Truth: For movement larger than 1 mm, we move the target with a high-precision sliding track (Mjunit MJ45N) which is capable of reporting the displacement at an accuracy of 0.01 mm. For subtle vibration, we obtain the ground truth readings from the vibration calibrator at an accuracy of ±1 μm.

Performance metric: The sensing metrics we focused on are displacement error and frequency error. We calculate the mean absolute error between the estimated values and the ground truths. For music recovery, vibration frequency is more important than the vibration amplitude.

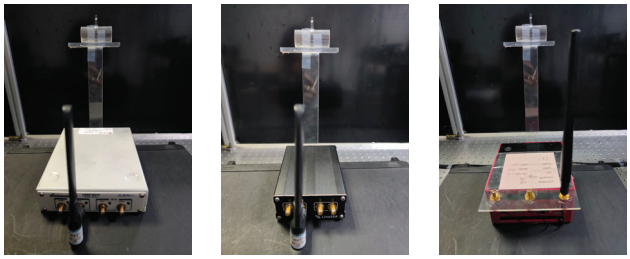

(a) USRP B210 (b) LimeSDR (c) Intel 5300

Figure 14: Two SDR devices and MiniPC with Intel 5300 WiFi card for conventional RF sensing.

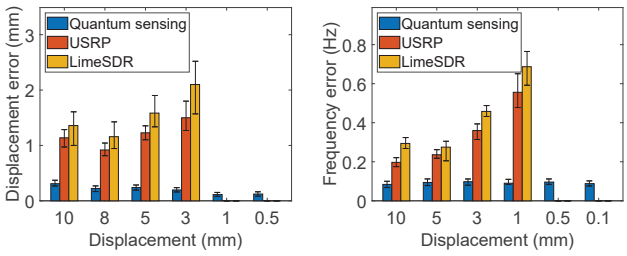

(a) Displacement error (b) Frequency error

Figure 15: Comparison of the sensing limits between quantum sensing system and conventional RF systems.

5.1.1 Comparison with conventional RF sensing systems. To compare the performance of the proposed quantum sensing with RF sensing, we adopt three different RF receivers commonly used in RF sensing, i.e., USRP B210, LimeSDR and Intel 5300 commodity WiFi card, which cost $3000, $400 and $10, respectively, as shown in Figure 14.

We first study the performance of RF sensing using USRP B210 and LimeSDR as the receiver at 2.4 GHz. For vibration

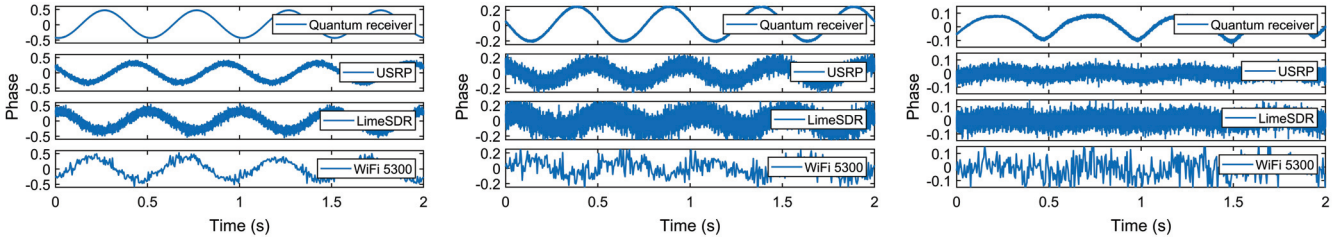

(a) Vibration displacement of 20 mm (b) Vibration displacement of 10 mm (c) Vibration displacement of 5 mm

Figure 16: Raw signal waveform comparison of quantum receiver, USRP, LimdSDR and Intel 5300 WiFi card when vibration displacement is 20 mm, 10 mm, and 5 mm.

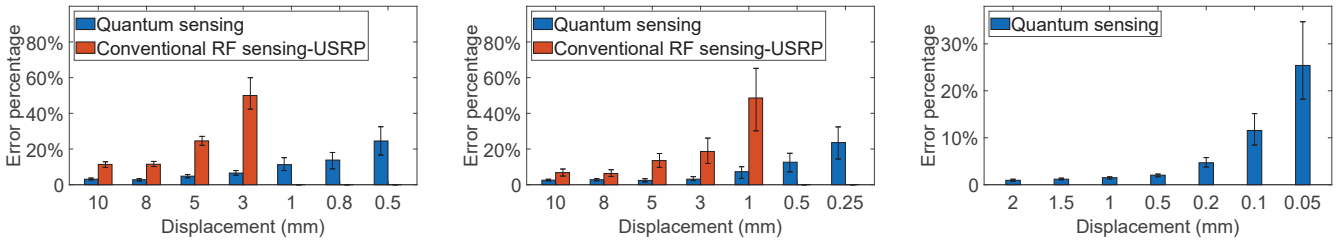

(a) Displacement error of 2.4 GHz (b) Displacement error of 5 GHz (c) Displacement error of 28 GHz

Figure 17: Evaluation of sensing limit using 2.4 GHz, 5 GHz and 28 GHz frequencies.

displacement under 1 mm, the vibration frequency is set as 30 Hz. For displacement larger than 1 mm, the vibration frequency is set as 5 Hz. As shown in Figure 15a, for a vibration displacement of 5 mm, quantum sensing, RF sensing based on USRP and LimeSDR achieve a displacement estimation error of 0.28 mm, 1.2 mm and 1.6 mm, respectively. As shown in Figure 15b, the frequency estimation errors of the proposed quantum sensing, RF sensing based on USRP and LimeSDR are 0.09 Hz, 0.24 Hz and 0.28 Hz, respectively. For vibrations smaller than 1 mm, RF sensing can no longer work, whereas the proposed quantum sensing still works well with an error less than 0.1 mm.

Next, we present a comparison of the raw signal captured at the quantum receiver, two SDR RF receivers and the commodity RF receiver (Intel 5300). The target vibration amplitude is set as 20 mm, 10 mm and 5 mm. As shown in Figure 16a, when the vibration amplitude is 20 mm, a clear vibration pattern can be observed at all four receivers. When the vibration amplitude is decreased to 5 mm in Figure 16c, we cannot see clear target vibration patterns at RF receivers. In contrast, a clear vibration pattern can still be observed at the quantum receiver. Note that all the signals presented are raw data without applying any filters.

We gradually decrease the vibration amplitude to obtain the sensing granularity, i.e., the minimum vibration amplitude when the error is still less than 30%. For amplitude sensing, the sensing granularity for commodity WiFi card and USRP B210 are both around 5 mm. In contrast, the granularity of quantum sensing can reach 0.5 mm which is much finer. For frequency sensing, the granularity of RF sensing is around 3 mm while the granularity of quantum sensing can reach 0.1 mm. We can thus conclude that quantum wireless sensing can improve the sensing granularity by more than 10 times at the frequency of 2.4 GHz.

5.1.2 Sensing granularity at different signal frequencies. In this section, we study if quantum sensing can work at other frequencies (e.g., 5 GHz and 28 GHz). The target vibration is varied from one centimeter to a few micrometers.

For displacement measurement, we show the estimation error at three frequencies in Figure 17a-17c. We can see that the sensing granularity of quantum wireless sensing for 2.4 GHz, 5 GHz, and 28 GHz signals is 0.5 mm, 0.25 mm, and 0.05 mm, respectively. In contrast, the sensing granularity of conventional RF sensing at 2.4 GHz and 5 GHz is 5 mm and 3 mm. Note that our USRP B210 platform can only support receiving signals in the frequency range of 70 MHz - 6 GHz. While it is difficult for one RF receiver to effectively capture RF signals in a large frequency range, one quantum receiver can cover frequencies from Megahertz to Terahertz due to completely different signal reception mechanism.

For frequency measurement, better performance can be achieved with quantum wireless sensing. The sensing granularity is further pushed to 0.1 mm, 0.05 mm and 0.01 mm for 2.4 GHz, 5 GHz, and 28 GHz signals, achieving 20 times granularity improvement. Based on this benchmark experiment, we show that even centimeter-wavelength signal (e.g.,

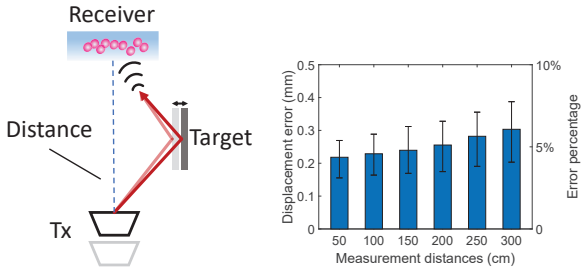

(a) Setup (b) Impact of distance

Figure 18: Experiment setup and impact of distance.

WiFi) can be used to sense subtle sub-millimeter vibration of a speaker to "sense" music in Section 5.2.1.

5.1.3 Impact of distance. We further investigate the impact of distance between transmitter and receiver on sensing accuracy. We show the experiment setup in Figure 18a. The vibration displacement and frequency are set to 5 mm and 20 Hz. We vary the distance between the signal transmitter and the vapor cell from 50 cm to 300 cm at a step size of 50 cm. The target is placed 1 m away from the LoS path. Figure 18b shows that our system is able to achieve an average error of 0.3 mm at a distance of 3 m. For a distance within 2 m, the average error is 0.25 mm.

5.1.4 Impact of obstacle on signal propagation path. In this experiment, we study the impact of obstacle on quantum wireless sensing. The vibration frequency and displacement of target are set as 20 Hz and 0.8 mm. We place obstacles made of four different materials, i.e., cardboard, wood, plastic and glass as shown in Figure 19 to block the signal propagation path between the transmitter antenna and target. As shown in Figure 20, the obstacle only causes a small increase of 0.01 *mm* - 0.05 *mm* (corresponding to a percentage of 1.25% - 6.25%) on displacement errors. This is because although the obstacle causes signal attenuation, owing to the high sensitivity of quantum wireless sensing, the performance is only slightly affected.

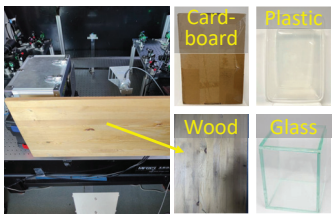

Figure 19: Sensing in the presence of obstacles.

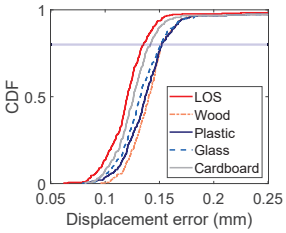

Figure 20: Impact of obstacles.

5.1.5 Sensing with commodity WiFi as transmitter. Note that as WiFi channel is 20 MHz and quantum receiver only listens to a much smaller frequency band, the amount of power captured at the quantum receiver is much smaller than the total WiFi power available. In this section, we want to see if the quantum receiver can use the very small portion of power captured from real WiFi packets for sensing. We conduct experiment using Intel 5300 WiFi card as the transmitter. Intel 5300 card is set to operate at channel 1 (2.412 GHz) with a bandwidth of 20 MHz. The interval of packet transmission is set as 10 ms. The small metal plate serves as the target.

As shown in Figure 21, we can see that even by just capturing a very small portion of power from WiFi transmissions, we can still achieve accurate vibration sensing. The achieved average error for vibration frequency sensing is 0.3 Hz (1.5%) which is still lower than the performance achieved with conventional WiFi sensing (3.5%). We want to point out that the channel size a quantum receiver is capable of listening to is being progressively increased in the last few years [10, 41] and we expect an even better sensing performance in the future with this trend.

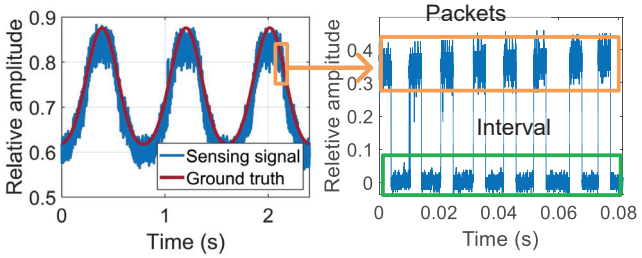

Figure 21: Sensing signal variation pattern and WiFi packets (zoomed in).

5.1.6 Impact of ambient RF interference. We further study the impact of ambient RF interference. We let our quantum receiver listen to RF signal at 2.412 GHz. As shown in Figure 22, we place two RF signal transmitters (one WiFi and one Bluetooth) near the vapor cell to create RF interference. The WiFi and Bluetooth interference are transmitted at 2.427 GHz and 2.402 GHz, respectively. The vibration displacement and frequency are set as 0.8 mm and 20 Hz.

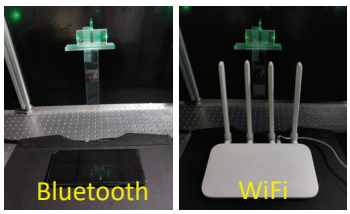

Figure 22: Sensing in the presence of interference signals.

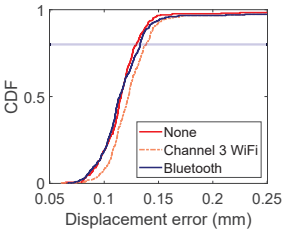

Figure 23: Impact of RF interference signals.

As shown in Figure 23, even though the frequency of the ambient RF signal is close to the sensing frequency, our system is affected very little. This is because Rydberg atoms are only sensitive to the electromagnetic wave in a small

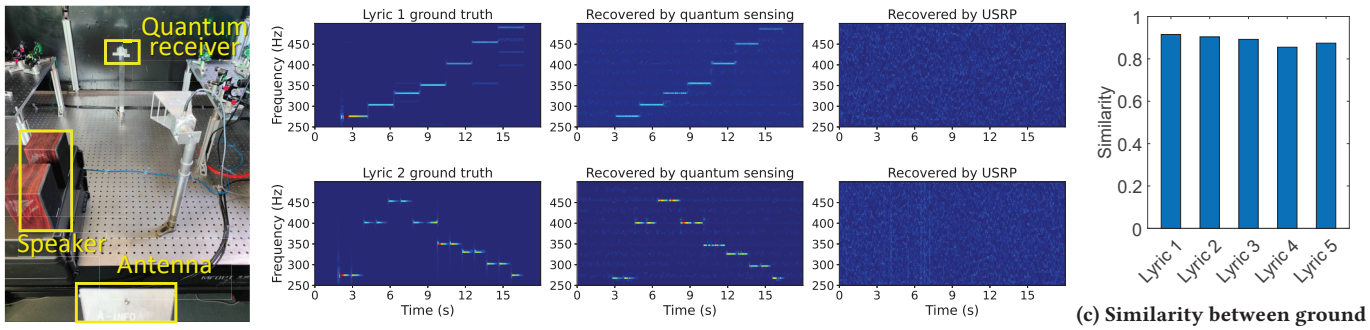

(a) Experiment setup

(b) Spectrum of sound and recovered sound by quantum sensing and USRP

(c) Similarity between ground truth and recovered sound

Figure 24: Experiment setup and results of sound sensing.

frequency range. Therefore, the chance of being interfered is small. Quantum receiver can thus resist interference in complex electromagnetic environments.

5.2 Case studies

In this section, we evaluate the performance of quantum wireless sensing in real-life applications.

5.2.1 Using centimeter wave to sense sub-millimeter vibration of a speaker. In RF sensing, a 2.4 GHz signal with a wavelength of 12 cm is capable of sensing millimeter-level motions. In this application, we show that quantum wireless sensing is capable of breaking this limit and pushing the sensing granularity to sub-millimeter level. Leveraging this finer granularity, we show that quantum wireless sensing can capture the subtle vibration of the speaker to "listen to" music. Previously this could only be achieved with higher-frequency millimeter wave signals [28, 32].

As shown in Figure 24a, a Philips SPA20 USB speaker with a small power of 3.5 W is placed on the desk. We employ 2.4 GHz signals for sensing, and Cs atoms in a vapor cell as the receiver. We play the seven basic music notes (i.e., do, re, mi, fa, so, la, and si) in the frequency range of 261 Hz to 494 Hz and the other four lyrics (Twinkle twinkle little star, For Elise, London bridge and Bingo). We plot the time-frequency spectrum of the speaker vibration when playing seven notes and Twinkle twinkle little star in Figure 24b (left: ground truth). We can see that our system can recover the sound the speaker is playing accurately purely through quantum wireless sensing. This can be used to record sound in a noisy environment. In contrast, conventional RF sensing using USRP B210 fails to sense the speaker vibration under the same setup as quantum wireless sensing, as shown in Figure 24b (right).

To quantify the performance of audio recovery of the five lyrics, we calculate the similarity between the original sound and recovered sound using cross-correlation of audio frequencies [49]. Figure 24c shows the results. Compared with direct recording using a microphone (93.7%), the achieved average similarity using the proposed quantum wireless sensing is only slightly worse (88.8%). The demo video for music sound recovery through quantum vibration sensing can be found at https://youtu.be/Do45Pa2fD6c.

5.2.2 Using millimeter wave to sense micrometer-level vibration. In this section, we further push the sensing granularity to micrometer level using millimeter-wave signals. One example of micrometer-level motion is the vibration of a bottle of water induced by a low-power USB speaker or human walking.

As shown in Figure 25a, a plastic bottle with water is placed on the table, and the speaker is placed 0.7 m from the bottle. We employ a Philips SPA20 USB speaker with a power of 3.5 W for our experiment. The volume level of the speaker is set as 50%. We play English words (i.e., one, two, three) using the speaker. In this experiment, we use 28 GHz RF signals for quantum wireless sensing. We extract the time-frequency spectrum of the signal captured at the quantum receiver, as shown in Figure 25b. By capturing the extremely subtle μm-level vibration of the bottle, we are able to restore the sound of the words from the speaker. As shown in Figure 25b, the recovered words match the ground truth well. The recovered sound can also be found at https://youtu.be/e4ALp8iYiTc.

We employ another interesting application to demonstrate the fine granularity of quantum wireless sensing. We use quantum wireless sensing to detect whether a person enters the room based on the subtle vibration induced at a water bottle on a table in the room. In this experiment, we let a person walk into the room. One 500 ml plastic bottle with water is placed on the desk. The desk is around 1 m from the door. When the person enters the room, human walking induces very subtle vibration (micrometer level) of the bottle. We extract the time-frequency spectrum of the signal captured at the quantum receiver, as shown in Figure 26b. We can see that the person enters the room at timestamp 1.8 s and stops

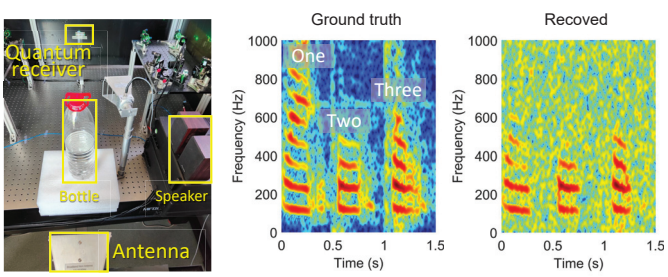

(a) Experiment setup (b) Spectrum results

Figure 25: Sense subtle micrometer-level vibration induced by speaker to recover words (i.e., one, two and three).

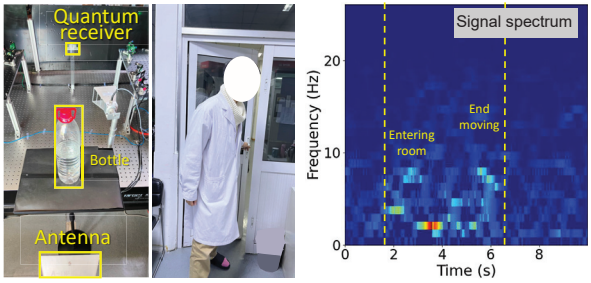

(a) Experiment setup (b) Spectrum result

Figure 26: Sense object' micrometer-level subtle vibration induced by human walking.

walking at 6.4 s. These timestamps match the ground truth captured using a video camera well. It can also be seen that human walking-induced bottle vibration contains multiple low-frequency components. We recruited 5 volunteers (2 females and 3 males) with a weight in the range of 50 kg to 85 kg. 100% detection accuracy can be achieved for all the 5 volunteers. Even for the female with the lightest weight of 50 kg, the induced vibration can still be accurately detected, demonstrating the superior performance of quantum wireless sensing. We believe more information such as the material of the floor and walking pattern may be extracted from the spectrum if proper machine learning models are applied.

6 RELATED WORK

Conventional RF sensing. A lot of research effort has been devoted to sensing humans and objects using RF signals. A large range of RF sensing applications have been developed, ranging from fine-grained vibration sensing [28, 54] and human vital sign monitoring [5, 61] to coarse-grained gesture tracking [42, 47] and daily activity recognition [34, 51]. A large variety of wireless technologies are utilized for sensing, including WiFi [4, 42, 61], bluetooth [40, 43], RFID [12, 15, 27], LoRa [13, 14, 54, 58], UWB [16, 59, 60] and FMCW radar [6, 7, 26, 55]. The signal frequency ranges from hundreds of megahertzs to tens of gigahertzs. However, the sensing granularity is fundamentally limited by hardware thermal noise generated at electronic components. For example, low-frequency WiFi signals cannot sense sub-millimeter motions. High-frequency signals are employed to achieve higher sensing granularity. However, the penetration capability of high frequency signals is weaker and the hardware cost is usually higher.

Quantum technology. Quantum technology is based on quantum mechanics and is new compared to RF technologies. In 1980, Paul Benioff proposed a quantum mechanical model of the Turing machine [8]. In 1998, the first two-qubit quantum computer which could perform computations was created [17]. Wiesner et. al introduced the concept of quantum conjugate coding showing the potential of quantum cryptography in 1992 [9]. Quantum technology was also used to design quantum network stack and link layer protocols [30][18][31]. In addition to these works, researchers discovered that Rydberg atoms could be used for communication and sensing in recent years [21, 29, 38, 56]. For quantum communication [44], it needs to send qubits from one quantum node to another. By creating quantum entangled qubits, information can be transmitted between remote quantum nodes. For quantum sensing, existing works aim at capturing the information of micro subjects such as molecules [21, 56]. The typical examples are atomic vapor magnetometers and atomic clocks [19]. Different from these works, this paper is the first to utilize quantum receiver and RF signals for sensing macro subjects such as human and daily objects.

7 DISCUSSIONS

In this section, we discuss the advantages and disadvantages of quantum wireless sensing. We compare it with conventional wireless sensing on the following aspects: size of frequency band, system noise, sensing sensitivity, system working frequency, and device cost/size.

Size of frequency band. The quantum receiver only listens to a narrow band once at a time and there are both advantage and disadvantage for this small band. The clear advantage is that as the quantum receiver only listens to a small band, it will not be interfered by adjacent channels. The disadvantage is that listening to a narrower band leads to lower received signal power and accordingly a smaller sensing range.

System noise. For conventional wireless sensing systems, electronic components such as mixers, amplifiers, and analog-to-digital converters (ADCs) all unavoidably introduce thermal noise. In contrast, a quantum receiver induces much smaller noise. The major source of noise comes from the photodetector adopted. The noise of a photodector consists

of thermal noise and shot noise. The thermal noise of a photodector is usually orders of magnitude smaller than the thermal noise of an RF amplifier. The shot noise is even smaller than the thermal noise.

Sensing granularity. Owing to smaller noise, quantum wireless sensing can improve the sensing granularity of conventional RF sensing by more than 10 times. On the other hand, higher sensing granularity also means quantum wireless sensing can be more easily interfered by non-target movements. Confining quantum wireless sensing only within the area of interest is an exciting direction to explore.

System working frequency. Conventional RF receivers are designed to receive signals in a particular frequency range. Even the antenna needs to be redesigned in order to efficiently receive signals in different frequency ranges. For example, while WiFi adopts dipole antennas, coil antennas is used to receive lower frequency signals. In quantum wireless sensing, one quantum receiver can receive RF signals of different frequencies by simply triggering the electrons to different energy levels. One quantum receiver can cover the frequency from a few Megahertz to tens of Terahertz.

Device cost and size. Quantum systems are still in the early stage of research and development. It is predicted that with further advances in laser miniaturization and integrated photonics, the size of the quantum receiver could be made much smaller [21]. We believe the price of quantum systems will also decrease dramatically. Take cesium clocks which contain lasers and Cs atoms in a vapor cell as an example. The size of today's cesium clocks is just 1% of the size of the first-generation design. The cost has been decreased from tens of thousands dollars to a few hundred dollars.

Future work: We demonstrate that quantum receiver can achieve a much finer granularity compared to conventional wireless sensing. We believe this finer granularity can enable exciting new applications. For example, while conventional WiFi sensing can only support hand tracking, quantum WiFi sensing may be used for finger tracking. We believe quantum wireless sensing has the potential to move one step forward to enable extremely fine-grained sweat and urine tests when high-frequency signals (e.g., Terahertz) are used.

8 CONCLUSION

In this paper, we present a new sensing modality, i.e., quantum wireless sensing for the first time. We reveal the underlying principle and design the first quantum wireless sensing system in the world. We show the superior performance of quantum wireless sensing compared to conventional RF sensing. We envision quantum wireless sensing can significantly improve the sensing performance in every aspect and also enable exciting new applications.

ACKNOWLEDGMENTS

This work is partially supported by the Beijing Nova Program (20220484138), the Beijing Natural Science Foundation (L223034), the National Natural Science Foundation of China (No. 62172394, No. 62072450), the Youth Innovation Promotion Association, Chinese Academy of Sciences (No. 2020109), the National Natural Science Foundation of China A3 Foresight Program (No.62061146001), the EU Horizon 2020 research and innovation programme IDEA-FAST (No. 853981).

A APPENDIX

A.1 Quantum defect

Table 1 below lists quantum defects with different angular momentum quantum numbers (i.e., S, P, D, F) and electron spin quantum numbers (i.e.,1/2, 3/2, 5/2, 7/2).

Table 1: Quantum defect of Cs atoms.

Energy level	δ_l
$nS_{1/2}$	4.04935665
$nP_{1/2}$	3.59158950
$nP_{3/2}$	3.559058
$nD_{3/2}$	2.475365
$nD_{5/2}$	2.46631524
$nF_{5/2}$	0.03341424
$nF_{7/2}$	0.033537

A.2 Calculation of energy level difference corresponding to RF signal frequency.

For 5 GHz frequency signal, the transition between energy levels $l_1 = 52D_{5/2}$ and $l_2 = 53P_{3/2}$ of Cs atom can be calculated as:

$$\begin{aligned} f_{l_1 \to l_2} &= \frac{|E_{l_2} - E_{l_1}|}{h} = cRy\left|\frac{1}{(53-\delta_{l_2})^2} - \frac{1}{(52-\delta_{l_1})^2}\right| \\ &= 3\times 10^8 \cdot 1.097 \times 10^7 \cdot \left|\frac{1}{(53-3.559)^2} - \frac{1}{(52-2.466)^2}\right| \\ &= 5\ GHz, \end{aligned} \tag{10}$$

For 28 GHz frequency signal, the transition between energy levels $l_1 = 61D_{5/2}$ and $l_2 = 63P_{1/2}$ of Cs atom can be calculated as:

$$\begin{aligned} f_{l_1 \to l_2} &= \frac{|E_{l_2} - E_{l_1}|}{h} = cRy\left|\frac{1}{(63-\delta_{l_2})^2} - \frac{1}{(61-\delta_{l_1})^2}\right| \\ &= 3\times 10^8 \cdot 1.097 \times 10^7 \cdot \left|\frac{1}{(63-3.592)^2} - \frac{1}{(61-2.466)^2}\right| \\ &= 28\ GHz. \end{aligned} \tag{11}$$

REFERENCES

[1] 2011. WiFi Intel 5300 CSI tool. https://dhalperi.github.io/linux-80211n-csitool/.

[2] 2022. USRP B210. https://www.ettus.com/all-products/UB210-KIT/ .Accessed:2022-09-20.

[3] C S Adams, J D Pritchard, and J P Shaffer. 2019. Rydberg atom quantum technologies. *Journal of Physics B: Atomic, Molecular and Optical Physics* 53, 1 (dec 2019), 012002.

[4] Fadel Adib and Dina Katabi. 2013. See through Walls with WiFi!. In *Proceedings of the ACM SIGCOMM 2013 Conference on SIGCOMM* (Hong Kong, China) *(SIGCOMM '13)*. Association for Computing Machinery, New York, NY, USA, 75–86.

[5] Fadel Adib, Hongzi Mao, Zachary Kabelac, Dina Katabi, and Robert C Miller. 2015. Smart homes that monitor breathing and heart rate. In *Proceedings of the 33rd annual ACM conference on human factors in computing systems*. 837–846.

[6] Fadel M. Adib, Chen-Yu Hsu, Hongzi Mao, Dina Katabi, and Frédo Durand. 2015. Capturing the human figure through a wall. *ACM Transactions on Graphics (TOG)* 34 (2015), 1 – 13.

[7] Fadel M. Adib, Zachary Kabelac, and Dina Katabi. 2015. Multi-Person Localization via RF Body Reflections. In *NSDI*.

[8] Paul Benioff. 1980. The computer as a physical system: A microscopic quantum mechanical Hamiltonian model of computers as represented by Turing machines. *Journal of statistical physics* 22, 5 (1980), 563–591.

[9] Charles H Bennett, François Bessette, Gilles Brassard, Louis Salvail, and John Smolin. 1992. Experimental quantum cryptography. *Journal of cryptology* 5, 1 (1992), 3–28.

[10] Stephanie M Bohaichuk, Donald Booth, Kent Nickerson, Harry Tai, and James P Shaffer. 2022. Origins of rydberg-atom electrometer transient response and its impact on radio-frequency pulse sensing. *Physical Review Applied* 18, 3 (2022), 034030.

[11] Julien Bourgeois and Wolfgang Minker. 2009. *Time-domain beamforming and blind source separation: speech input in the car environment*. Springer.

[12] Yanling Bu, Lei Xie, Yinyin Gong, Chuyu Wang, Lei Yang, Jia Liu, and Sanglu Lu. 2022. RF-Dial: Rigid Motion Tracking and Touch Gesture Detection for Interaction via RFID Tags. *IEEE Transactions on Mobile Computing* 21, 3 (2022), 1061–1080.

[13] Zhaoxin Chang, Fusang Zhang, Jie Xiong, Junqi Ma, Beihong Jin, and Daqing Zhang. 2022. Sensor-free Soil Moisture Sensing Using LoRa Signals. *Proceedings of the ACM on Interactive, Mobile, Wearable and Ubiquitous Technologies* 6, 2 (2022), 1–27.

[14] Lili Chen, Jie Xiong, Xiaojiang Chen, Sunghoon Ivan Lee, Kai Chen, Dianhe Han, Dingyi Fang, Zhanyong Tang, and Zongge Wang. 2019. WideSee: towards wide-area contactless wireless sensing. *Proceedings of the 17th Conference on Embedded Networked Sensor Systems* (2019).

[15] Lili Chen, Jie Xiong, Xiaojiang Chen, Sunghoon Ivan Lee, Daqing Zhang, Tao Yan, and Dingyi Fang. 2019. LungTrack: Towards Contactless and Zero Dead-Zone Respiration Monitoring with Commodity RFIDs. *Proc. ACM Interact. Mob. Wearable Ubiquitous Technol.* 3 (2019), 79:1–79:22.

[16] Weiyan Chen, Fusang Zhang, Tao Gu, Kexing Zhou, Zixuan Huo, and Daqing Zhang. 2022. Constructing Floor Plan through Smoke Using Ultra Wideband Radar. *Proc. ACM Interact. Mob. Wearable Ubiquitous Technol.* 5, 4, Article 147 (dec 2022), 29 pages.

[17] Isaac L Chuang, Neil Gershenfeld, and Mark Kubinec. 1998. Experimental implementation of fast quantum searching. *Physical review letters* 80, 15 (1998), 3408.

[18] Axel Dahlberg, Matthew Skrzypczyk, Tim Coopmans, Leon Wubben, Filip Rozpundefineddek, Matteo Pompili, Arian Stolk, Przemysław Pawełczak, Robert Knegjens, Julio de Oliveira Filho, Ronald Hanson, and Stephanie Wehner. 2019. A Link Layer Protocol for Quantum Networks. In *Proceedings of the ACM Special Interest Group on Data Communication* (Beijing, China) *(SIGCOMM '19)*. Association for Computing Machinery, New York, NY, USA, 159–173.

[19] C. L. Degen, F. Reinhard, and P. Cappellaro. 2017. Quantum sensing. *Rev. Mod. Phys.* 89 (Jul 2017), 39 pages. Issue 3.

[20] Robert Dougherty. 2004. Advanced time-domain beamforming techniques. In *10th AIAA/CEAS Aeroacoustics Conference*. 2955.

[21] Charles T. Fancher, David R. Scherer, Marc C. St. John, and Bonnie L. Schmittberger Marlow. 2021. Rydberg Atom Electric Field Sensors for Communications and Sensing. *IEEE Transactions on Quantum Engineering* 2 (2021), 1–13. https://doi.org/10.1109/TQE.2021.3065227

[22] Chao Feng, Jie Xiong, Liqiong Chang, Ju Wang, Xiaojiang Chen, Dingyi Fang, and Zhanyong Tang. 2019. Wimi: Target material identification with commodity wi-fi devices. In *2019 IEEE 39th International Conference on Distributed Computing Systems (ICDCS)*. IEEE, 700–710.

[23] Thomas Gallagher. 2006. *Rydberg Atoms*. Springer New York, New York, NY, 235–245. https://doi.org/10.1007/978-0-387-26308-3_14

[24] Walter Gander, Gene H. Golub, and Rolf Strebel. 1994. Least-squares fitting of circles and ellipses. *BIT Numerical Mathematics* 34, 4 (1994), 558–578.

[25] Nicolas Gisin and Rob Thew. 2007. Quantum communication. *Nature photonics* 1, 3 (2007), 165–171.

[26] Unsoo Ha, Salah Assana, and Fadel Adib. 2020. Contactless Seismocardiography via Deep Learning Radars. In *Proceedings of the 26th Annual International Conference on Mobile Computing and Networking (MobiCom '20)*. Association for Computing Machinery, Article 62, 14 pages.

[27] Unsoo Ha, Junshan Leng, Alaa Khaddaj, and Fadel Adib. 2020. Food and Liquid Sensing in Practical Environments using RFIDs. In *17th USENIX Symposium on Networked Systems Design and Implementation (NSDI 20)*. USENIX Association, Santa Clara, CA, 1083–1100. https://www.usenix.org/conference/nsdi20/presentation/ha

[28] Chengkun Jiang, Junchen Guo, Yuan He, Meng Jin, Shuai Li, and Yunhao Liu. 2020. MmVib: Micrometer-Level Vibration Measurement with Mmwave Radar. In *Proceedings of the 26th Annual International Conference on Mobile Computing and Networking* (London, United Kingdom) *(MobiCom '20)*. Association for Computing Machinery, New York, NY, USA, Article 45, 13 pages.

[29] Yuechun Jiao, Xiaoxuan Han, Jiabei Fan, Georg Raithel, Jianming Zhao, and Suotang Jia. 2019. Atom-based receiver for amplitude-modulated baseband signals in high-frequency radio communication. *Applied Physics Express* 12, 12 (2019), 126002.

[30] Minsung Kim, Davide Venturelli, and Kyle Jamieson. 2019. Leveraging Quantum Annealing for Large MIMO Processing in Centralized Radio Access Networks. In *Proceedings of the ACM Special Interest Group on Data Communication* (Beijing, China) *(SIGCOMM '19)*. Association for Computing Machinery, New York, NY, USA, 241–255.

[31] Minsung Kim, Davide Venturelli, John Kaewell, and Kyle Jamieson. 2022. Warm-Started Quantum Sphere Decoding via Reverse Annealing for Massive IoT Connectivity. In *Proceedings of the 28th Annual International Conference on Mobile Computing And Networking* (Sydney, NSW, Australia) *(MobiCom '22)*. Association for Computing Machinery, New York, NY, USA, 1–14. https://doi.org/10.1145/3495243.3560516

[32] Huining Li, Chenhan Xu, Aditya Singh Rathore, Zhengxiong Li, Hanbin Zhang, Chen Song, Kun Wang, Lu Su, Feng Lin, Kui Ren, and Wenyao Xu. 2020. VocalPrint: exploring a resilient and secure voice authentication via mmWave biometric interrogation. *Proceedings of the 18th Conference on Embedded Networked Sensor Systems* (2020).

[33] Yang Li, Dan Wu, Jie Zhang, Xuhai Xu, Yaxiong Xie, Tao Gu, and Daqing Zhang. 2022. DiverSense: Maximizing Wi-Fi Sensing Range Leveraging Signal Diversity. *Proc. ACM Interact. Mob. Wearable Ubiquitous Technol.* 6, 2, Article 94 (jul 2022), 28 pages. https://doi.org/10.

1145/3536393

[34] Jian Liu, Hongbo Liu, Yingying Chen, Yan Wang, and Chen Wang. 2020. Wireless Sensing for Human Activity: A Survey. *IEEE Communications Surveys Tutorials* 22, 3 (2020), 1629–1645. https://doi.org/10.1109/COMST.2019.2934489

[35] C.J. Lorenzen and K. Niemax. 1984. Precise quantum defects of nS, nP and nD Levels in Cs I. *Zeitschrift für Physik A Atoms and Nuclei* 315 (1984), 127–133.

[36] Yongsen Ma, Gang Zhou, and Shuangquan Wang. 2019. WiFi Sensing with Channel State Information: A Survey. *ACM Comput. Surv.* 52, 3, Article 46 (jun 2019), 36 pages.

[37] N David Mermin. 2007. *Quantum computer science: an introduction.* Cambridge University Press.

[38] David H Meyer, Kevin C Cox, Fredrik K Fatemi, and Paul D Kunz. 2018. Digital communication with Rydberg atoms and amplitude-modulated microwave fields. *Applied Physics Letters* 112, 21 (2018), 211108.

[39] Moritz Müller, Jins de Jong, Maran van Heesch, Benno Overeinder, and Roland van Rijswijk-Deij. 2020. Retrofitting Post-Quantum Cryptography in Internet Protocols: A Case Study of DNSSEC. *SIGCOMM Comput. Commun. Rev.* 50, 4 (oct 2020), 49–57.

[40] F. Naya, H. Noma, R. Ohmura, and K. Kogure. 2005. Bluetooth-based indoor proximity sensing for nursing context awareness. In *Ninth IEEE International Symposium on Wearable Computers (ISWC'05)*. 212–213.

[41] Nikunjkumar Prajapati, Andrew P Rotunno, Samuel Berweger, Matthew T Simons, Alexandra B Artusio-Glimpse, Stephen D Voran, and Christopher L Holloway. 2022. TV and video game streaming with a quantum receiver: A study on a Rydberg atom-based receiver's bandwidth and reception clarity. *AVS Quantum Science* 4, 3 (2022), 035001.

[42] Qifan Pu, Sidhant Gupta, Shyamnath Gollakota, and Shwetak Patel. 2013. Whole-Home Gesture Recognition Using Wireless Signals. In *Proceedings of the 19th Annual International Conference on Mobile Computing and Networking (MobiCom '13)*. Association for Computing Machinery, 27–38.

[43] Ziyuan Pu, Meixin Zhu, Wenxiang Li, Zhiyong Cui, Xiaoyu Guo, and Yinhai Wang. 2021. Monitoring Public Transit Ridership Flow by Passively Sensing Wi-Fi and Bluetooth Mobile Devices. *IEEE Internet of Things Journal* 8, 1 (2021), 474–486.

[44] Ji-Gang Ren, Ping Xu, Hai-Lin Yong, Liang Zhang, Sheng-Kai Liao, Juan Yin, Wei-Yue Liu, Wen-Qi Cai, Meng Yang, Li Li, et al. 2017. Ground-to-satellite quantum teleportation. *Nature* 549, 7670 (2017), 70–73.

[45] Jonathon A Sedlacek, Arne Schwettmann, Harald Kübler, Robert Löw, Tilman Pfau, and James P Shaffer. 2012. Microwave electrometry with Rydberg atoms in a vapour cell using bright atomic resonances. *Nature Physics* 8, 11 (2012), 819–824.

[46] Shouqian Shi and Chen Qian. 2020. Concurrent Entanglement Routing for Quantum Networks: Model and Designs. In *Proceedings of the Annual Conference of the ACM Special Interest Group on Data Communication on the Applications, Technologies, Architectures, and Protocols for Computer Communication (SIGCOMM '20)*. Association for Computing Machinery, New York, NY, USA, 62–75.

[47] Li Sun, Souvik Sen, Dimitrios Koutsonikolas, and Kyu-Han Kim. 2015. WiDraw: Enabling Hands-Free Drawing in the Air on Commodity WiFi Devices. In *Proceedings of the 21st Annual International Conference on Mobile Computing and Networking* (Paris, France) *(MobiCom '15)*. Association for Computing Machinery, New York, NY, USA, 77–89.

[48] Sheng Tan, Yili Ren, Jie Yang, and Yingying Chen. 2022. Commodity WiFi Sensing in Ten Years: Status, Challenges, and Opportunities. *IEEE Internet of Things Journal* 9, 18 (2022), 17832–17843.

[49] Chuyu Wang, Lei Xie, Yuancan Lin, Wei Wang, Yingying Chen, Yanling Bu, Kai Zhang, and Sanglu Lu. 2022. Thru-the-wall Eavesdropping on Loudspeakers via RFID by Capturing Sub-mm Level Vibration. *Proceedings of the ACM on Interactive, Mobile, Wearable and Ubiquitous Technologies* 5, 4 (Dec. 2022), 182:1–182:25.

[50] Jingxian Wang, Junbo Zhang, Rajarshi Saha, Haojian Jin, and Swarun Kumar. 2019. Pushing the Range Limits of Commercial Passive RFIDs. In *16th USENIX Symposium on Networked Systems Design and Implementation (NSDI 19)*. USENIX Association, Boston, MA, 301–316.

[51] Wei Wang, Alex X. Liu, Muhammad Shahzad, Kang Ling, and Sanglu Lu. 2015. Understanding and Modeling of WiFi Signal Based Human Activity Recognition *(MobiCom '15)*. Association for Computing Machinery, New York, NY, USA, 65–76. https://doi.org/10.1145/2789168.2790093

[52] Binbin Xie, Jie Xiong, Xiaojiang Chen, Eugene Chai, Liyao Li, Zhanyong Tang, and Dingyi Fang. 2019. Tagtag: material sensing with commodity rfid. In *Proceedings of the 17th Conference on Embedded Networked Sensor Systems*. 338–350.

[53] Binbin Xie, Jie Xiong, Xiaojiang Chen, and Dingyi Fang. 2020. Exploring Commodity RFID for Contactless Sub-Millimeter Vibration Sensing. In *Proceedings of the 18th Conference on Embedded Networked Sensor Systems (SenSys '20)*. Association for Computing Machinery, 15–27.

[54] Binbin Xie, Yuqing Yin, and Jie Xiong. 2021. Pushing the Limits of Long Range Wireless Sensing with LoRa. *Proceedings of the ACM on Interactive, Mobile, Wearable and Ubiquitous Technologies* 5 (2021), 1 – 21.

[55] Chenhan Xu, Zhengxiong Li, Hanbin Zhang, Aditya Singh Rathore, Huining Li, Chen Song, Kun Wang, and Wenyao Xu. 2019. WaveEar: Exploring a mmWave-based Noise-resistant Speech Sensing for Voice-User Interface. *Proceedings of the 17th Annual International Conference on Mobile Systems, Applications, and Services* (2019).

[56] Chung-Jui Yu, Stephen von Kugelgen, Daniel W. Laorenza, and Danna E. Freedman. 2021. A Molecular Approach to Quantum Sensing. *ACS Central Science* 7, 5 (2021), 712–723. https://doi.org/10.1021/acscentsci.0c00737 arXiv:https://doi.org/10.1021/acscentsci.0c00737 PMID: 34079892.

[57] Daqing Zhang, Fusang Zhang, Dan Wu, Jie Xiong, and Kai Niu. 2021. *Fresnel Zone Based Theories for Contactless Sensing.* Springer International Publishing, Cham, 145–164.

[58] Fusang Zhang, Zhaoxin Chang, Kai Niu, Jie Xiong, Beihong Jin, Qin Lv, and Daqing Zhang. 2020. Exploring LoRa for Long-Range Through-Wall Sensing. *Proc. ACM Interact. Mob. Wearable Ubiquitous Technol.* 4, 2, Article 68 (June 2020), 27 pages.

[59] Fusang Zhang, Zhaoxin Chang, Jie Xiong, Junqi Ma, Jiazhi Ni, Wenbo Zhang, Beihong Jin, and Daqing Zhang. 2023. Embracing Consumer-level UWB-equipped Devices for Fine-grained Wireless Sensing. *Proceedings of the ACM on Interactive, Mobile, Wearable and Ubiquitous Technologies* 6, 4 (2023), 1–27.

[60] Fusang Zhang, Jie Xiong, Zhaoxin Chang, Junqi Ma, and Daqing Zhang. 2022. Mobi2Sense: Empowering Wireless Sensing with Mobility. In *Proceedings of the 28th Annual International Conference on Mobile Computing and Networking*.

[61] Fusang Zhang, Daqing Zhang, Jie Xiong, Hao Wang, Kai Niu, Beihong Jin, and Yuxiang Wang. 2018. From Fresnel Diffraction Model to Fine-Grained Human Respiration Sensing with Commodity Wi-Fi Devices. *Proc. ACM Interact. Mob. Wearable Ubiquitous Technol.* 2, 1, Article 53 (mar 2018), 23 pages. https://doi.org/10.1145/3191785

[62] Mingmin Zhao, Yonglong Tian, Hang Zhao, Mohammad Abu Alsheikh, Tianhong Li, Rumen Hristov, Zachary Kabelac, Dina Katabi, and Antonio Torralba. 2018. RF-Based 3D Skeletons. In *Proceedings of the 2018 Conference of the ACM Special Interest Group on Data Communication (SIGCOMM '18)*. Association for Computing Machinery, New York, NY, USA, 267–281.